

ELECTRICAL STUDIES OF Cu WIRE INTERCONNECTIONS IN ELECTRONIC PACKAGES UPON HIGH-TEMPERATURE STORAGE

¹T. Joseph Sahaya Anand, S. ¹Shariza, ²Chua Kok Yau, ¹A.R.M. Warikh, ¹Kok-Tee Lau, ²Lim Boon Huat

¹Faculty of Manufacturing Engineering, Universiti Teknikal Malaysia Melaka (UTeM), Melaka, Malaysia.

²Infineon Technologies (Malaysia) Sdn. Bhd., Melaka, Malaysia.

Presented at International Symposium on Research in Innovation and Sustainability 2019 (ISoRIS '19) 28 -29 August 2019

ABSTRACT: Electrical performance of wire bond interconnection in electronic packages relates closely to the functionality of the microchip during a performance in any application. During high-temperature storage (HTS), Cu-Al intermetallic compound (IMC) forms due to interfacial diffusion between Cu wire and Al metallization. Heat treatment enhances the growth of the Cu-Al IMC leading to an increase in the thickness of the IMC layer. In this paper, we report the electrical studies and the interfacial microstructure of the thermostatically bonded Cu wire to Al metallization bond pad bonded at 280 °C and annealed for 1000 hours. Samples were studied for their morphology via transmission electron microscopy - energy dispersive X-ray analysis (TEM-EDX) while the electrical resistivity of the packages was studied via the current-voltage curve measurements. The experiment results are summarized as: (i) an increase of HTS duration increases the thickness of the Cu-Al IMC interface layer; and (ii) an increase of the Cu-Al IMC layer thickness increases the electrical resistivity of the electronic package. These studies provide insights into how these parameters can contribute to the development of materials and devices for improved reliability.

Index Terms: Electrical studies, High-temperature storage (HTS), Intermetallic compound (IMC), Wire bond

1. INTRODUCTION

Copper (Cu) wire bonding has gained scores of attention in recent years and has been widely employed in micro and nanoscale electronic devices by the existing semiconductor production and packaging industry [1-3]. It plays a significant role because the copper wire has better thermal and electrical conductivity properties [4] and much slower and more stable intermetallic compounds (IMC) growth with aluminum (Al) bond pads compared to the conventional gold (Au) wire [5]. In addition, there is very little void formation in the Al-Cu system compared to the Al-Au system. This leads to lower electrical contact resistance, less heat generation, and better reliability and device performance, compared to Au/Al bonds [6]. Besides, the properties of Cu which have higher mechanical strength than Au results in a better manufacturing process control in terms of looping profiles control (for ultra-fine pitch wire bonding) as well as lesser sagging wire quality issue [7]. Nowadays, Cu wire has become a common interconnection material in wire bonding packages with numerous reports seen published in the last decade [1-8].

During service, wire-bonded packages may experience elevated temperatures, resulting in overgrowth of IMCs and voids at the IMC interface. An overgrowth of IMCs and voids may potentially increase the risk of brittle fracture of the system leading to a degradation in the quality of the IMCs' performances [9, 10]. This growth may persist up to a stage that may possibly detriment the electrical and mechanical properties of the package, directly affecting its functionality and operational life [8]. The quality of interconnects in the semiconductor packages needs to be more robust in order to withstand severe conditions and longer life. It is not practical to directly examine the interfacial behavior of bonds of the packages that physically undergo a long duration of their service. Hence, annealing otherwise known as HTS is employed in experiments to imitate and accelerate the chemical reactions that take place during long durations of service life.

Previous research has shown that the electrical resistance of the Cu-Al IMC is significantly affected by factors: (i) the

thickness and (ii) microstructure, as well as (iii) the phase of the Cu-Al interface [11]. In view of the phase diagram of Cu-Al in Figure 1, various phases of IMC can possibly form [12].

The Cu-Al phase identified from the phase diagram are α -Al, CuAl₂ (θ), CuAl (η_2), Cu₄Al₃ (ζ_2), Cu₃Al₂ (δ), Cu₉Al₄ (γ_1), and FCC-Cu for temperature below 350°C. Any of these phases are expected to be present in the IMC for the samples tested in this report.

The IMC diffusion-reaction is known to take place in an elevated temperature environment. However, to our knowledge, almost no reports have been found to study the electrical properties of wire bonds in electronic packages after long hours of HTS. Considering the correlation between the above factors (i.e., (i) the thickness, (ii) microstructure, and (iii) the phase of the Cu-Al interface) and the reliability of the package in its application, and electrical properties of the package were studied.

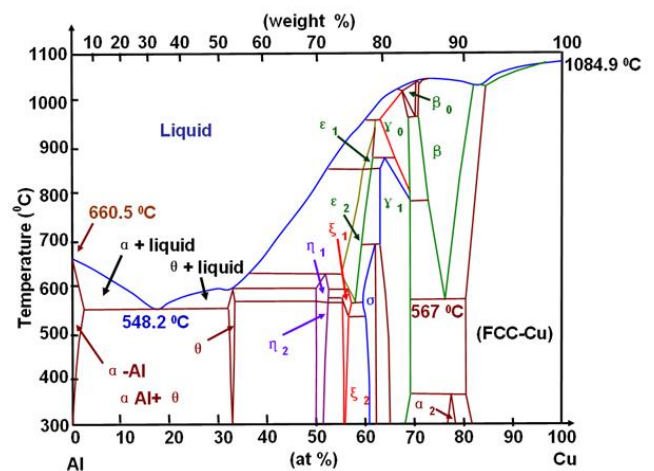


Figure 1: The Cu-Al equilibrium phase diagram [12].

In this paper, we are the first to study and report the effect of prolonged HTS treatment on the electrical resistivity of electronic packages and its relationship to the microstructure of the wire bond IMC layer.

2. EXPERIMENTAL PROCEDURE

Diode microchips with pure Al bond pad metallization were first transferred from wafer to lead frame by die bonding process. Then the samples were thermostatically bonded at 280°C with Cu wire (purity of 99.999%) with a fine-tuned flow of inert forming gas to hinder Cu free air ball (FAB) oxidation. The wire bonding process was carried out on a commercially available Shinkawa® ACB-35. These samples were then encapsulated using an epoxy mould compound.

To understand the effects of annealing on the microstructure of the IMC and the electrical resistivity of the packages, the packages were subjected to the static annealing treatment under nitrogen gas flow in the oven to protect the sample from oxidation. Three states for characterization were chosen: (i) as-bonded (not subjected to HTS) (ii) intermediately aged, where IMC layers have formed, and (iii) highly aged. State (ii) and (iii) were achieved by HTS treatment at 175°C after 500 hours and 1000 hours respectively.

The electrical studies of the encapsulated samples were conducted via a current-voltage (I–V) analysis. 30 samples of each state were tested so that the test results would proximately satisfy a normal distribution. These diode samples were under forwarding bias with a voltage > 0.66 V, which was adjusted by a potential meter. A voltmeter and ammeter were connected in parallel and series to the diode samples, respectively. With this setup, the voltmeter records the biasing voltage; while the ammeter captures the corresponding current. Figure 2 shows the circuit diagram for the I-V analysis. The resistance of the samples was then obtained from the division of the difference of potential to passing current, according to Ohm's Law.

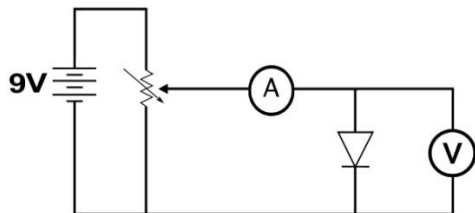


Figure 2: Circuit diagram for I-V analysis

To analyze the bonding interface, the mounting of the annealed and un-encapsulated sample was performed by molding a specimen from each state. Samples were further prepared with a mechanical cross-section which includes grinding and polishing prior to focus ion beam (FIB) lamella extraction for morphological studies. In FIB, a thin lamella with a thickness dimension of 0.1µm was extracted from the peripheral bonding interface consisting of Si, Al bond pad, and Cu ball bond. The lamellas were then inspected by the FEI TECNAI G2F20 system which is capable of Transmission Electron Microscope (TEM) and line scan Energy Dispersive X-ray (EDX). Thickness measurement and phase identification of the IMC layer were derived from the EDX spectrums.

3 RESULTS AND DISCUSSION

Figure 3(a) – 3(c) shows the box plot of the resistivity values of the samples at different HTS durations. The increase in resistance of the samples was due to the Cu-Al intermetallics interfacial diffusion-reaction that was induced by the HTS treatment at longer hours. This observation has also been reported in a larger scale material by [13] and is discussed further in the next paragraphs.

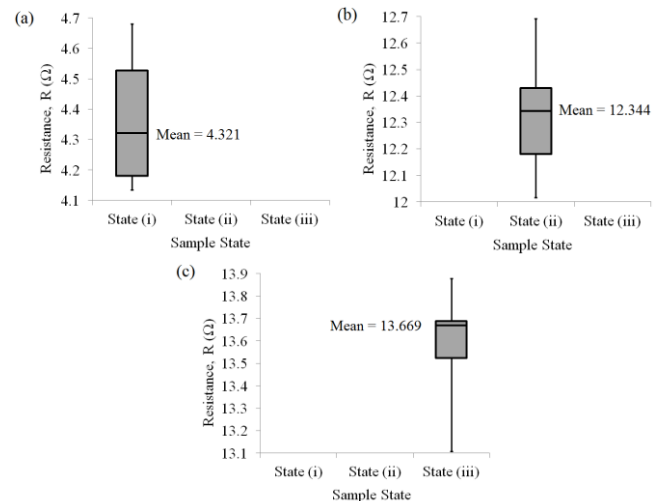


Figure 3(a)-3(c): Box plot of the resistivity values of the samples.

TEM photograph of the cross-section of the sample at its wire bond in the state (i) at the point where the EDX line scan was carried out (arrow direction) and its corresponding EDX composition profile are shown in Figure 4 and Figure 5, respectively.

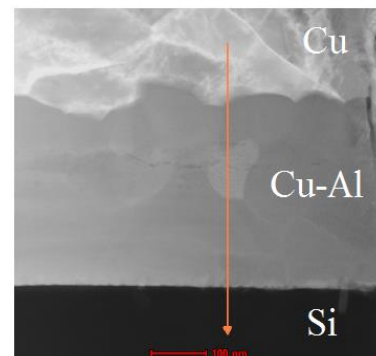


Figure 4: TEM photograph of wire bond cross-section in the state (i).

In Figure 4, a distinctive layer of Cu-Al IMC is observed. The Al bond pad is easily consumed completely in the early aging duration as agreed in [7] in which a Cu-rich Cu-Al IMC with 80 wt% Cu has formed. Referring to Figure 5 with reference to the Cu-Al phase diagram in Figure 1, the IMC layer formed is of $\delta + \gamma_1$ phase that has a thickness of approximately 328 nm.

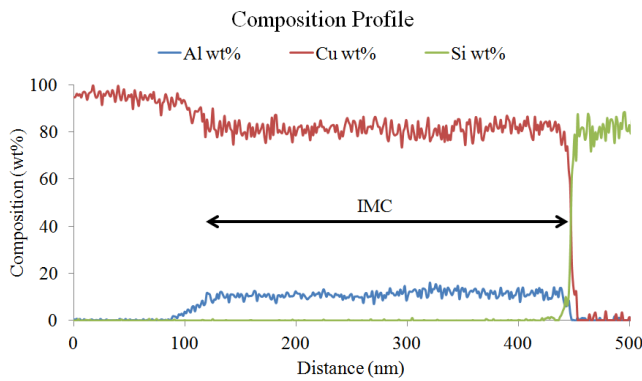


Figure 5: EDX composition profile for wire bond cross-section in the state (i).

Figure 6 shows the TEM photograph of the cross-section of the sample at its wire bond in the state (iii) at the point where the EDX line scan was carried out (arrow direction) and its corresponding EDX composition profile is shown in Figure 6. In Figure 6, three (3) distinctive layers of Cu-Al IMC can be observed. It is clearly seen from the colour tone of each IMC layer labeled as "1", "2" and "3" in the figure.

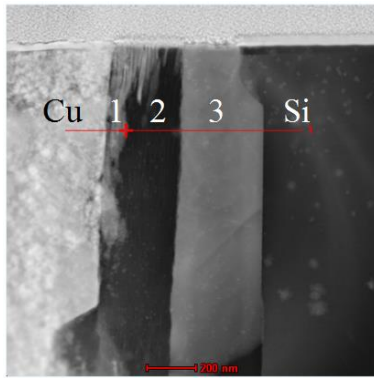


Figure 6: TEM photograph of wire bond cross-section in the state (iii).

Referring to Figure 7 with reference to the Cu-Al phase diagram in Figure 1, the IMC layer formed and its thickness are identified as follows:

- (a) Layer 1: $\theta + \eta_2$ phase with 59 wt% Cu at a thickness of 58 nm.
- (b) Layer 2: $\alpha\text{-Al} + \theta$ phase with 5 wt% Cu at a thickness of 211 nm.
- (c) Layer 3: $\theta + \eta_2$ phase with 60 wt% Cu at a thickness of 313 nm.

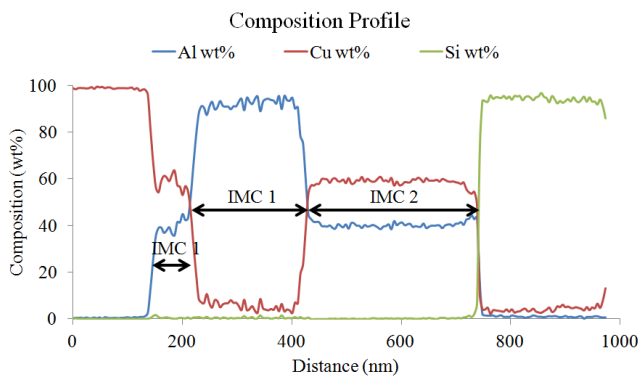


Figure 7: EDX composition profile for wire bond cross-section in the state (iii).

In Figure 6, there are distinctive rod-like features in IMC layer 1. To identify the compound of this structure, an EDX line scan was carried out across three (3) rod-like features in the said layer. A magnified TEM photograph of IMC layer 1 and the position of the EDX line scan are shown in Figure 8.

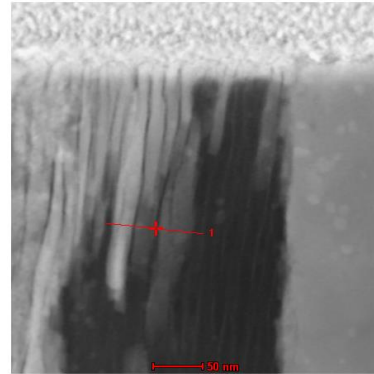


Figure 8: Magnified TEM photograph of layer 1 in the state (iii).

Figure 9 shows the EDX composition profile obtained for the specific area. It was observed that the main constituents of the rod-like features were Cu and Al elements. Therefore, the rod-like features were confirmed to be an IMC formation which corresponds to a mixture of $\alpha\text{-Al} + \theta$ phase with 30-50% wt% Cu. In addition, the presence of the θ phase in the region with rod shape feature was validated by NBD measurement, as shown in Figure 10.

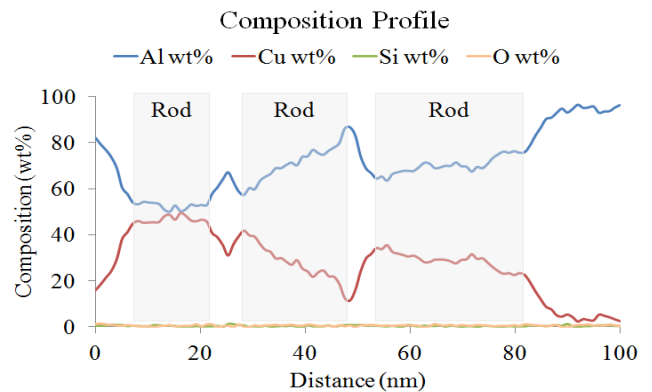


Figure 9: EDX composition file for rod-like features in IMC layer 1.

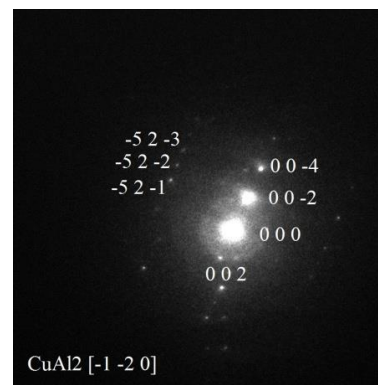


Figure 10: NBD diffraction pattern that matched the diffraction from plane [-1 -2 0] of θ phase.

The formation of θ phase IMC rod-like structures also indicates that diffusion in Cu–Al system is dominated by Cu.

When Cu diffusion is faster than Al diffusion through the IMCs, Cu atoms reach the Al pad and react with Al to form θ phase first [14]. This supports the observations in Figure 6 whereby the location of the θ phase IMC is at layer 1, near the Cu material. The growth of layer 1 IMC is then followed by

layer 2 and layer 3 IMC as observed in Figure 6. These observations also imply that at a highly thermal aged state (i.e. state (iii)), the development of IMC rods consisting of Cu-Al results in a reduced number of free electrons available and hence, decreasing the electrical conductivity causing an increase in the electrical resistance of the samples. A similar observation has been reported by [11].

Table 1: Summary of Total IMC Thickness, Phase Identification and Mean Resistivity Value

Sample state	Total IMC thickness (nm)	IMC Phase Identification	%wt Cu	Mean Resistivity Value (Ω)
State (i)	328	IMC: $\delta + \gamma_1$	80%	4.321
State (iii)	582	IMC 1: $\theta + \eta_2$ Thickness: 58 nm	59%	13.669
		IMC 2: α -Al + θ Thickness: 211 nm	5%	
		IMC 3: $\theta + \eta_2$ Thickness: 313 nm	60%	

The electrical resistance changes are believed to be caused by Cu-Al intermetallic growth at the ball bond. This is also agreed by [15]. The electrical resistivity of the Cu-Al IMCs increases during the annealing process, resulting from the formation and growth of the Cu–Al IMC layer, because the IMC layer has much higher electrical resistivity, compared with those of Cu and Al [13].

During the wire bonding and HTS process, thermally activated reactive diffusion leads to the nucleation and growth of the IMC at the metal-metal (i.e. Cu-Al) interface as suggested by [16]. An occurrence like this, the IMCs continue to grow due to the induced mobility of copper atoms to diffuse into the interface upon longer hours of HTS. As a result, the thickness of the IMC increases. The results of variations in the specific resistance of the samples with increased thickness of the IMCs are shown in Table 1. As can be seen, experimental results show that with the increase in annealing time, the thickness of the IMC grew, the electrical resistance also increased, and electrical conductivity decreased.

4. CONCLUSION

Because Samples of Cu wire thermostatically bonded on pure Al bond pad metallization were successfully synthesized at 280°C with the supply of forming gas. Samples were then treated to HTS of durations of 500 hours and 1000 hours. Results show that there are variations in the specific resistance of the samples with increased thickness of the IMCs. With the increase of annealing time, the IMC layer thickness increases, resulting in an increase in the electrical resistivity of the Cu-Al IMC. A longer HTS duration was found to enhance the interfacial diffusion of the Cu-Al IMC. Line-scan EDX reveals that the IMC actually consists of an interdiffusion zone and a distinctive thin layer of intermetallic phase, whereby in highly thermal aged samples, more than one phase of Cu-Al IMC was formed. The results

from these studies together with further reliability studies, it provides insights into the development of materials and devices for improved reliability.

REFERENCES

1. Hirohiko Endoh and Takuya Naoe, "Copper wire bonding package decapsulation using the anodic protection method," *Microelectronics Reliability*, vol. 55, 2015, pp. 207-212.
2. Subramani Manoharan, Chandradip Patel, Patrick McCluskey, and Michael Pecht, "Effective decapsulation of copper wire-bonded microelectronic devices for reliability assessment," *Microelectronics Reliability*, vol. 84, 2018, pp. 197-207.
3. A. Mazloun-Nejadari, G. Khatibi, B. Czerny, M. Lederer, J. Nicolics, and L. Weiss, "Reliability of Cu wire bonds in microelectronic packages," *Microelectronics Reliability*, vol. 74, 2017, pp. 147-154.
4. Chauhan P.S., Choubey A., Zhong Z., and Pecht M.G., "Copper wire bonding," in *Copper Wire Bonding*, New York: Springer, 2014.
5. Subramani Manoharan, Chandradip Patel, Stevan Hunter, and Patrick McCluskey, "Influence of initial shear strength on time-to-failure of copper (Cu) wire bonds in thermal aging condition," *Additional Conferences (Device Packaging, HiTEC, HiTEN, & CICMT)*, pp. 32-38, 2018.
6. Zhong Z.W., "Overview of wire bonding using copper wire or insulated wire," *Microelectronics Reliability*, vol. 51, 2011, pp. 4-12.
7. Chien-Pan Liu, Shouou-Jinn Chang, Yen-Fu Liu, and Wei-Shou Chen, "Cu-Al interfacial formation and

- kinetic growth behavior during HTS reliability test,” *Journal of Materials Processing Tech.*, vol. 267, 2019, pp. 90-102.
8. Lee Cher Chia, Chua Kok Yau, T. Joseph Sahaya Anand, S. Shariza, and Mohamad Ridzuan Bin Jamli, “Modelling of wire bonding Cu-Al intermetallic formation growth towards interfacial stress,” presented at IEEE 19th Electronics Packaging Technology Conference (EPTC), Singapore, December 6-9, 2017.
 9. Hsien-Chie Cheng, Ching-Feng Yu and Wen-Hwa Chen, “First-principles density functional calculation of mechanical, thermodynamic and electronic properties of CuIn and Cu₂In crystals,” *Journal of Alloys and Compounds*, vol. 546, 2013, pp. 286-295.
 10. Kunmo Chu, Yoonchul Sohn and Changyool Moon, “A comparative study of Cu/Sn/Cu and Ni/Sn/Ni solder joints for low temperature stable transient liquid phase bonding,” *Scripta Materialia*, vol. 109, 2015, pp. 113-117.
 11. Soheil Tavassoli, Mehrdad Abbasi, and Ramin Tahavvori, “Controlling of IMCs layers formation sequence, bond strength and electrical resistance in Al-Cu bimetal compound casting process,” *Materials and Design*, vol. 108, 2016, pp. 343-353.
 12. Kathlene N. Reeve, Iver E. Anderson, and Carol A. Handwerker, “Nucleation and growth of Cu-Al intermetallics in Al-modified Sn-Cu and Sn-Ag-Cu lead-free solder alloys,” *Journal of Electronic Materials*, vol. 44(3), 2015, pp. 842-866.
 13. Jian Zhang, Bin-Hao Wang, Guo-Hong Chen, Ruo-Min Wang, Chun-Hui Miao, Zhi-Xiang Zheng, and Wen-Ming Tang, “Formation and growth of Cu-Al IMCs and their effect on electrical property of electroplated Cu/Al laminar composites,” *Transactions of Nonferrous Metals Society of China*, vol. 26, no. 12, 2016, pp. 3283-3291.
 14. Hui Xu, Ivy Qin, Horst Clauberg, Bob Chylak, and Viola L. Acoff, “New observation of nanoscale interfacial evolution in micro Cu-Al wire bonds by in-situ high resolution TEM study,” *Scripta Materialia*, vol. 115, 2016, pp. 1-5.
 15. M.D. Hook, S. Hunter, and M. Mayer, “Deriving lifetime predictions for wire bonds at high temperatures,” *Microelectronics Reliability*, vol. 88-90, 2018, pp. 1124-1129.
 16. M. Guerdane, “Self-diffusion in intermetallic AlAu₄: Molecular dynamics study down to temperatures relevant to wire bonding,” *Computational Materials Science*, vol. 129, 2017, pp. 13-23.
-